

Glueball Matrix Elements on Anisotropic Lattices*

Y. Chen^{ab}, S.-J. Dong^a, T. Draper^a, I. Horváth^a, F.-X. Lee^{cd}, N. Mathur^a, C. Morningstar^e, M. Peardon^f, S. Tamhankar^a, B.L. Young^g, and J.-B. Zhang^h

^aDepartment of Physics and Astronomy, University of Kentucky, Lexington, KY 40506, USA

^bInstitute of High Energy Physics, Chinese Academy of Sciences, Beijing 100039, P. R. China

^cCenter for Nuclear Studies, Dept. of Physics, George Washington Univ., Washington, DC 20052, USA

^dJefferson Lab, 12000 Jefferson Avenue, Newport News, VA 23606, USA

^eDepartment of Physics, Carnegie Mellon University, Pittsburgh, PA 15213, USA

^fSchool of Mathematics, Trinity College, Dublin 2, Ireland

^gDepartment of Physics, Carnegie Mellon University, Pittsburgh, PA 15213, USA

^hCSSM and Department of Physics, Univ. of Adelaide, Adelaide, SA 5005, Australia

The glueball-to-vacuum matrix elements of local gluonic operators in scalar, tensor, and pseudoscalar channels are investigated numerically on several anisotropic lattices with the spatial lattice spacing in the range $0.1fm - 0.2fm$. These matrix elements are needed to predict the glueball branching ratios in J/ψ radiative decays which will help to identify the glueball states in experiments. Two types of improved local gluonic operators are constructed for a self-consistent check, and the finite volume effects are also studied. The lattice spacing dependence of our results is very small and the continuum limits are reliably extrapolated.

1. Introduction

Glueballs, predicted by QCD, are so exotic from the point of view of the naive quark model that their existence will be a confirmation of QCD. Extensive numerical studies have been carried out to simulate the glueball spectrum and resulted that the low-lying glueballs are in the mass range $1 - 3$ GeV, which suggests that the J/ψ radiative decays are the ideal hunting ground for glueballs. There are several possible glueball candidates in the final states of J/ψ radiative decays, however, more criteria are needed for their unambiguous identifications, one of which might be the partial widths of J/ψ radiative decays into glueballs. To estimate these partial widths, the vacuum-to-glueball transition matrix elements(TME) of local gluonic operators should

be derived first.

The techniques of lattice simulations in the glueball sector have been substantially improved in the past decade. Inspired by the success of anisotropic lattice techniques in the simulations of the glueball spectrum [1] and as a continuation of former studies [2,3], this work is devoted to the numerical study of TME on anisotropic lattices with tadpole-improved gauge action.

2. LOCAL GLUONIC OPERATORS

The TME computed in this work are $\langle 0|S(x)|0^{++}\rangle$, $\langle 0|T_{\mu\nu}(x)|2^{++}\rangle$, and $\langle 0|P(x)|0^{-+}\rangle$, where $|J^{PC}\rangle$ refers to the glueball state with the quantum number J^{PC} , and the local operators $S(x)$, $T_{\mu\nu}$, and $P(x)$ are trace anomaly $g^2 Tr G_{\mu\nu} G_{\mu\nu}(x)$, the energy-momentum tensor $g^2 Tr(G_{\mu\alpha}(x)G_{\alpha\nu}(x) - \frac{1}{4}g_{\mu\nu}G^2(x))$, and the topological charge density $g^2 \epsilon_{\mu\nu\rho\sigma} Tr G_{\mu\nu}(x)G_{\rho\sigma}(x)$,

*Presented by S.-J. Dong.

Table 1
The simulation parameters.

β	ξ	u_s	$a_s(fm)$	$L^3 \times T$	#Meas.
2.4	5	0.409	0.222(2)	$8^3 \times 40$	20000
				$12^3 \times 64$	10000
				$16^3 \times 80$	10000
2.6	5	0.438	0.176(1)	$12^3 \times 64$	8600
2.7	5	0.451	0.156(1)	$12^3 \times 64$	10000
3.0	3	0.500	0.120(1)	$16^3 \times 48$	10000
3.2	3	0.521	0.101(1)	$24^3 \times 72$	7900

respectively ($G_{\mu\nu}(x)$ is the gauge field strength and g the gauge coupling). Two types of lattice local gluonic operators (Type-I and Type-II) are constructed in this work.

Type-I operators are linear combinations of a set of small Wilson loops according to the irreducible representations of the lattice symmetry group, namely, A_1^{++} , A_1^{+-} , E^{++} , and T_2^{++} [4]. Letting $O^R(x)$ be the local operators of specific quantum number R , the construction of Type-I operators can be expressed as

$$O^R(x) = \sum_i C_i^R \text{ReTr}(W_1^{(i)}(x) + \alpha W_2^{(i)}(x) + \dots), \quad (1)$$

where C_i^R are the combinational coefficients. Different Wilson loops W_1, W_2, \dots are included with proper factors α to improve the operator.

To construct Type-II operators, we define the lattice gauge field strength $\hat{F}_{\mu\nu}(x)$ as

$$\hat{F}_{\mu\nu}(x) = \text{Im} \langle f(u_s) P_{\mu\nu}(x) + g(u_s) R_{\mu\nu}(x) \rangle_c, \quad (2)$$

where $P_{\mu\nu}(x)$, and $R_{\mu\nu}(x)$ are respectively the plaquette and rectangle at x . $\langle \cdot \rangle_c$ means the clover average, $f(u_s)$ and $g(u_s)$ are factors including the tadpole parameter $u_s = ((1/3 \text{Tr} P_{ij}))^{1/4}$ and are chosen in a way that yields $\hat{F}_{\mu\nu}(x) = a_s^2(G_{\mu\nu}(x) + O(a_s^4))$ (a_s is the spatial lattice spacing). Proper combinations of $\text{Tr} \hat{F}_{\mu\nu}(x) \hat{F}_{\rho\sigma}(x)$ give the Type-II operators with reduced lattice artifacts.

There are seven matrix elements calculated in this work, which are denoted by (S,B), (S,E), (E,B), (E,E), (T,B), (T,E), and (PS). Here (,B) (or (,E)) means the operator is made up of color-magnetic (or color-electric) field, and (PS) refers to the pseudoscalar channel.

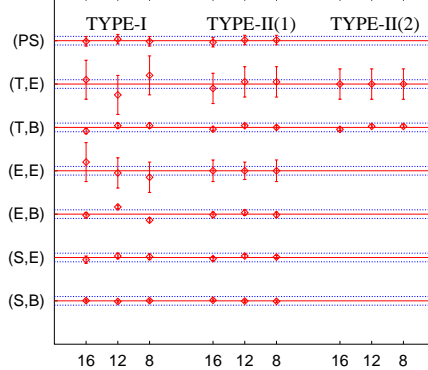


Figure 1. Finite-volume effects of matrix elements.

3. SIMULATION DETAILS AND RESULTS

Numerical simulations were carried out on anisotropic lattices with tadpole-improved gauge action [1]. Five independent simulations have been done with input parameter listed in Table. 1.

With the tadpole improvement, the local gluonic operators on the lattice are all improved to $O(a_s^4)$ (a_s is the spatial lattice spacing) at the tree level. With applying the variational method to the combinations of smeared Wilson loops with different prototypes [1], glueball states are obtained through correlators of smeared operators which have large overlaps with glueball states. Six independent runs were carried out, on lattices with spatial lattice spacings in the range $0.1 fm - 0.22 fm$, to measure the smeared-smeared correlators $C_{SS}(t)$ and smeared-local correlators $C_{SL}(t)$. The matrix elements are extracted by fitting $C_{SS}(t)$ and $C_{SL}(t)$ simultaneously using the correlated χ^2 method. The fit models are taken as

$$\begin{aligned} C_{SS}(t) &= X^2 e^{-Mt} \\ C_{SL}(t) &= XY e^{-Mt}, \end{aligned} \quad (3)$$

where X is the amplitude of the glueball operators, Y is the glueball-to-vacuum matrix element,

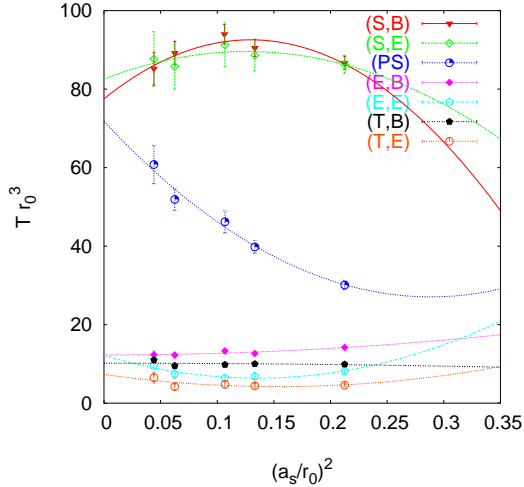


Figure 2. Continuum extrapolations of matrix elements of Type-I operators.

and M is the glueball mass.

The finite volume effects (FVE) of matrix elements are studied on lattices $8^3 \times 40$, $12^3 \times 64$, and $16^3 \times 80$ at $\beta = 2.4$, $\xi = 5$, and the results are shown in Fig. 1, where each point with a errorbar is the fractional change, $\delta_G(L) = 1 - f_G(L)/\bar{f}_G$, in the matrix elements (\bar{f}_G is the average value of the matrix elements of glueball G over the three lattice volumes, and $f_G(L)$ is the matrix element of glueball G measured on lattice $L^3 \times T$). The labels $L = 8, 12$, and 16 denote the different lattice volumes, and the labels along the vertical axis represent the matrix elements of the different local operators. To guide eyes, $\delta_G = 0$ and $\delta_G = \pm 0.02$ are also drawn in Fig. 1 with solid line and dash lines, respectively. All changes are statistically consistent with zero, indicating that systematic errors from FVE are negligible.

The simulated results of matrix elements at different lattice spacings are shown in Fig. 2 (Type-I operators) and Fig. 3 (Type-II operators), where a_s (in units of $r_0 \sim (410(20)MeV)^{-1}$, the hadronic scale parameter) dependences are observed. The matrix elements can be reliably extrapolated to the continuum limit by using the form $f(a_s/r_0) = Tr_0^3 + c_2(a_s/r_0)^2 + c_4(a_s/r_0)^4$, where Tr_0^3 , c_2 , and c_4 are best-fit parameters. We keep the a_s^2 term in the fitting model because there are residual $\alpha_s a_s^2$ artifacts in the gauge ac-

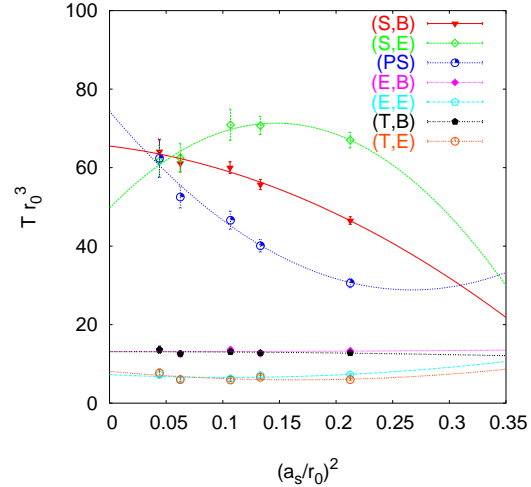


Figure 3. Continuum extrapolations of matrix elements of Type-II operators.

tion and some local operators. From the figures one can find that the Type-II operators exhibit better behaviors (for example, the matrix elements of T_2 and E representations coincide, as it should be when the rotational symmetry is restored in the continuum limit).

The physically available predictions will not be derived until the local gluonic operators are properly renormalized. The nonperturbative renormalization of these operators is in progress.

This work is supported by DOE Grants DE-FG05-84ER40154 and DE-FG02-02ER45967. Y. Chen is partly supported by NSFC (No.10075051, 12035040) and CAS (KJCX2-SW-N02).

REFERENCES

1. C. Morningstar and M. Peardon, Phys. Rev. D**56** (1997) 4043; Phys. Rev. D**60** (1999) 034509.
2. Y. Liang, K.F. Liu, B.A. Li, and S.J. Dong, Phys. Lett. B**307** (1993) 375.
3. S.J. Dong *et al*, Nucl. Phys. Proc. Suppl. **63** (1998) 254.
4. B. Berg and A. Billoire, Nucl. Phys. B**221** (1983) 109.